Assembly and function of cell surface structures of the thermoacidophilic archaeon Sulfolobus solfataricus

Zolghadr, Behnam

CHAPTER 4

Appendage-mediated surface adherence of *Sulfolobus solfataricus*

Behnam Zolghadr, Andreas Klingl, Andrea Koerdt, Arnold J.M. Driessen, Reinhard Rachel, and Sonja-Verena Albers

Journal of Bacteriology. (2010) 192: 104.

Abstract

Attachment of microorganisms to surfaces is a prerequisite for colonization and biofilm formation. The hyperthermophilic crenarchaeote *Sulfolobus solfataricus* was able to attach to a variety of surfaces such as glass, mica, pyrite and carbon-coated gold grids. Deletion mutant analysis showed that for initial attachment the presence of flagella and pili is essential. Attached cells produced extracellular polysaccharides containing mannose, galactose and N-acetylglucosamine. Genes possibly involved in the production of the extracellular polysaccharides were identified.

[#]B. Zolghadr and A. Klingl equally contributed to this paper.

INTRODUCTION

In microbiology, organisms are isolated from their natural habitat and typically cultivated in the laboratory as planktonic species. Though this method has been essential for understanding the concept of life, it remains unclear how microbial ecosystems operate. For bacteria it is well known that they are able to form large cellular communities with highly complex cellular interactions and symbiosis between different microbial or eukaryotic species. Biofilm formation is an essential component of such communities and studies have shown that bacteria within biofilms are physiologically different to planktonic ones (Watnick & Kolter, 2000, Watnick & Kolter, 1999). They can exhibit extensive networks of pili on their surface and produce and secrete extracellular polysaccharides, their growth rate is decreased and cells are much more resistant to physical stresses and antibiotics (Vu *et al.*, 2009).

The study of surface colonisation and cellular communities of archaea is crucial for understanding their ecological properties. The only detailed study showed that the hyperthermophilic *Archaeoglobus fulgidus* produced biofilms when challenged with heavy metals and pentachlorophenol (LaPaglia & Hartzell, 1997). *Pyrococcus furiosus* was able to adhere to different surfaces such as mica and carbon-coated gold grids and cells were connected via cable-like bundles of flagella (Nather *et al.*, 2006). *Methanopyrus kandleri* was shown to adhere to glass, however, *P. furiosus* could only colonize by attaching to *M. kandleri* cells using flagella and direct cell contacts (Schopf *et al.*, 2008).

Here we report on the function of cell surface appendages in initial attachment to surfaces of archaea using directed gene inactivation mutants. The crenarchaeote *Sulfolobus solfataricus* P2 is a thermoacidophile which grows optimally at 80^{o}C and pH values of 2-4 (Zillig *et al.*, 1980). *S. solfataricus* possesses cell surface structures such as flagella and UV induced pili (Albers & Pohlschroder, 2009, Albers *et al.*, 2006b). The flagella operon of *S. solfataricus* contains next to the structural subunit FlaB, four proteins of unknown function, the ATPase FlaI and the only integrale membrane protein FlaJ. Previously, we have isolated a Δ*flaJ* mutant which was non-flagellated and had lost its ability for surface motility on gelrite plates (Szabo *et al.*, 2007a). Recently, we described UV inducible pili in *S. solfataricus* that directed cellular aggregation after UV stress (Frols *et al.*, 2007). Deletion of the central ATPase, UpsE, responsible for pili assembly rendered cells devoid of pili and defective in cellular aggregation after UV treatment (Frols *et al.*, 2007). In this study wildtype cells and deletion strains were tested for their ability to attach to a variety of surfaces and the formed structures and extracellular material were analyzed.

RESULTS

Attachment of *S. solfataricus* to various surfaces

For initial attachment to different materials, we tested *S. solfataricus* P2 and *S. solfataricus* PBL2025, and the Δ*flaJ* and Δ*upsE* mutants derived from this strain. Carbon-coated gold grids were incubated in shaking cultures for 2 days in tryptone medium. PBL2025 adhered to the carbon-coated gold grids and some flagella and more straight pili were present (Figure 1A and C). In comparison only very few cells of the Δ*flaJ* (Figure 1B) and Δ*upsE* (Table 1) strains attached to the carbon grids, implying an important role for both the flagella and UV induced pili for this process. The same experiment was repeated with the addition of sulfur to the tryptone medium to mimic the natural habitat of *Sulfolobus* species. Considerably more PBL2025 cells were found attached to the carbon film compared to tryptone medium alone (Figure 1D). Moreover, the cells clustered around the sulfur particles (Figure 1E) and developed some extracellular sheet-like structure connecting the cells (Figure 1F). Other materials tested for attachment of cells were glass, pyrite, and mica, a layered aluminum silicate which forms extremely smooth and clean surfaces when cleaved with a razor blade (for overview see Table 1). *S. solfataricus* P2 and PBL2025 grew very differently on mica surfaces. PBL2025 formed microcolonies and produced very large thin layers of extracellular material in which cells were embedded (Figure 2A/B). *S. solfataricus* P2 formed a more regular, extended network of extracellular appendages containing some other material in between the structures (Figure 2C/D). As shown for carbon-coated grids, cells of Δ*flaJ* and Δ*upsE* were also unable to adhere to mica (data not shown). *S. solfataricus* P2 grew best on glass surfaces yielding more cells than on mica or carbon-coated grids. Obviously, the cells attached to the surfaces using flagella and pili (Figure 2E/F), but did not produce the extensive network of extracellular material and appendages as observed on mica. The Δ*flaJ* and Δ*upsE* strains were also not able to grow on glass (Table 1).

Analysis of extracellular material from attached cells

It is well known that extracellular proteins of *Sulfolobales* are glycosylated. Glucose, mannose, galactose and N-acetylglucosamine have previously been identified in the glycans of sugar-binding proteins (Elferink et al., 2001b). Moreover, the same sugars were found in extracellular polysaccharides that are produced mainly in the stationary growth phase of *S. solfataricus* MT3 and MTA4 (Nicolaus *et al.*, 2003). Therefore fluorescently labeled lectins were used to determine the nature of the extracellular material produced by the attached *S. solfataricus* cells. Glass slides were incubated for three days in shaking *S. solfataricus* P2 and PBL2025 cultures. After fixation the samples were incubated with fluorescently labeled lectins directed against terminal α-D-galactosyl residues (Isolectin-IB_4), α- or β-linked *N*-acetyl-D-glucosamine (GS-II), or α-

mannopyranosyl and α-glucopyranosyl residues (ConcanvalinA, ConA). In *S. solfataricus* P2 all three lectins reacted with the extracellular material indicating the presence of the different sugars recognized by the different lectins (Figure 3, A-H). ConA and isolectin-IB4 also bound to cells staining the cell envelope whereas GS-II only attached to the extracellular material. As shown by the scanning electron images (Figure 2), PBL2025 formed a more and dense appearing extracellular material, which was also visible by light microscopy (Figure 3, I-P). Also with PBL2025, all three lectins bound to the extracellular material; interestingly, and in contrast to *S. solfataricus* P2, the lectin GS-II also bound to the cell envelope. From this analysis it can be concluded that *Sulfolobus* strains produce extracellular polysaccharides (EPS) when attached to a glass surface.

TABLE 1. Different materials tested for attachment of *S. solfataricus* strains

	***S. solfataricus* Strains**			
Surface	P2	PBL2025	Δ*upsE*	Δ*flaJ*
Mica (Glimmer)	Growth on surface with many flagella and pili	Growth on surface with pili	No growth	No growth
Glass	Growth on surface; cells are connected with a mesh-wire of flagella/pili	Growth on surface. No pili and flagella visible.	No growth	No growth
Pyrite (FeS_2)	Growth on surface	No growth	No growth	No growth
Gold-Grids coated with carbon	Growth on surface with pili and flagella	Growth on surface with pili and flagella	Only very few cells present	Only very few cells present

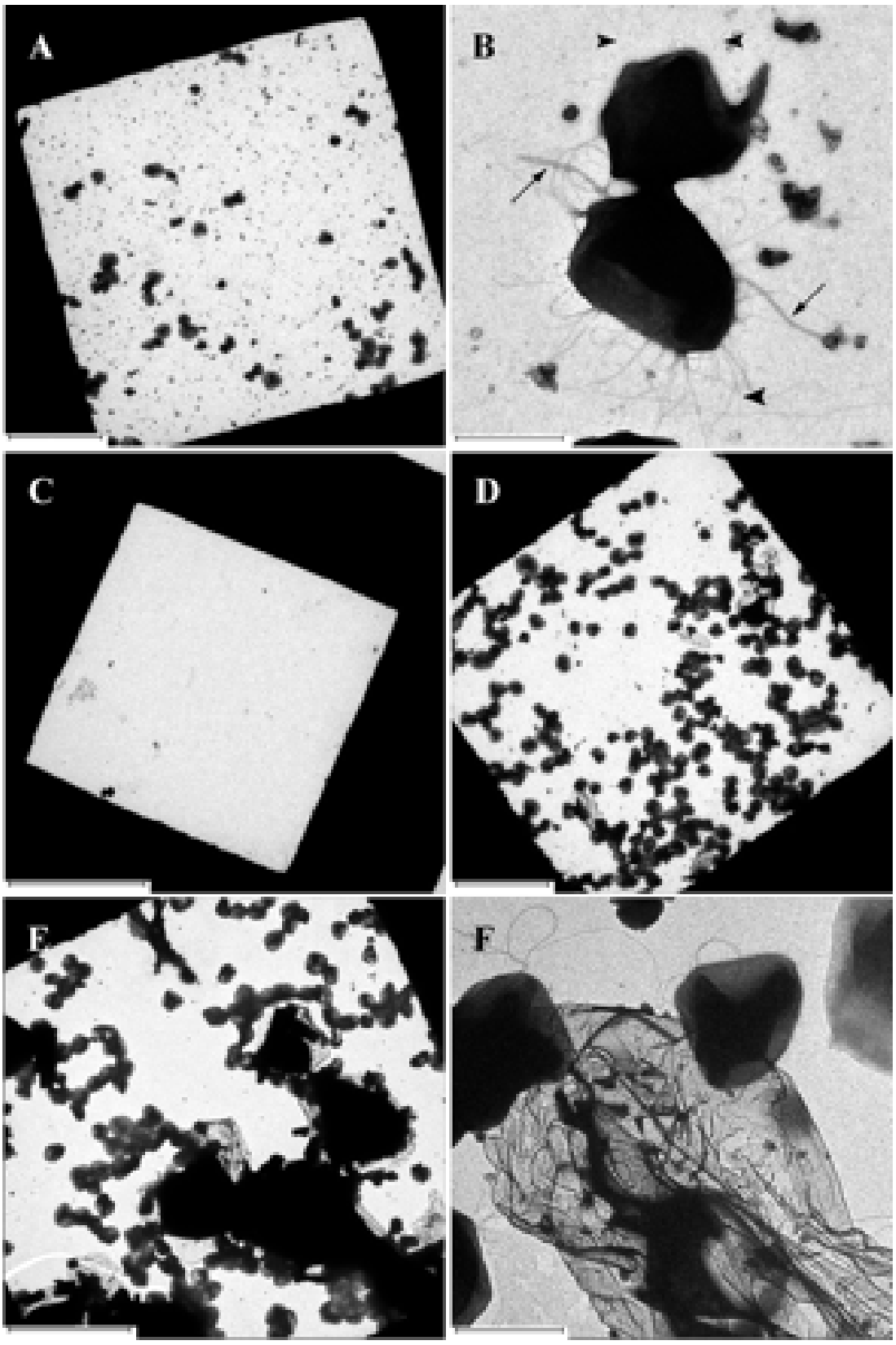

Figure 1. Attachment of strain PBL2025 to carbon-coated gold grids. Transmission electron micrographs of PBL2025 attached to carbon (A and B). At higher magnifications, flagella (arrows) and pili (arrow heads) could be detected (B). Δ*flaJ* was not able to adhere under these conditions (C). When sulfur was added to the medium, considerably more PBL2025 cells attached to the carbon film (D), adhere to the sulfur particles (E) and produced an extracellular sheet-like material (F). Bars: A, D, E: 10 µm; B, F: 1 µm; C: 20 µm

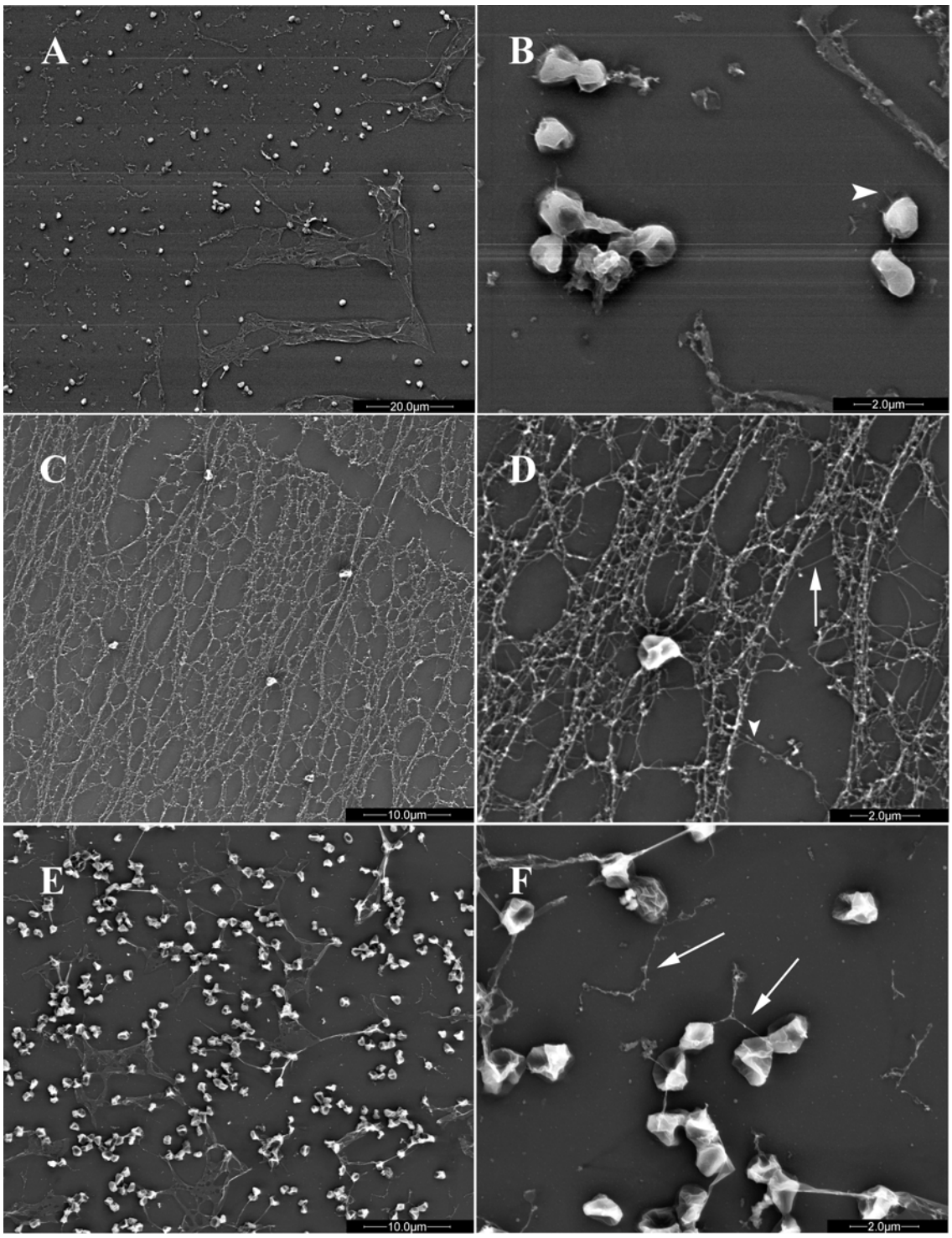

Figure 2. Attachment of *S. solfataricus* P2 and PBL2025 to mica and glass. PBL2025 attached to mica and produced extracellular sheet-like structures (A/B), whereas P2 adhered via an extensive network of flagella/pili (C/D; D: enlargement of C). Attachment of *S. solfataricus* P2 to glass was very different than to mica (E/F; F: enlargement of E). Pili (arrow heads) and flagella (arrows) are indicated in A-F. Bars: A: 20 µm; B, D, F: 2 µm; C, E: 10 µm

Analysis of differentially expressed genes in attached *S. solfataricus* P2 cells

As shown in Figure 2 attachment of *S.solfataricus* P2 and PBL2025 to mica resulted in diverse structures, especially the extracellular material formed had a different appearance. In contrast to *S. solfataricus* P2, strain PBL2025 lacks the genes SSO3004-3050 (Schelert *et al.*, 2004). This region includes a diverse set of genes possibly involved in sugar degradation and lipid metabolism (see Table 2) As the EPS produced by the two strains differed significantly, we explored whether the genes in the aforementioned region are involved in the production or modulation of EPS during growth of *Sulfolobales* on surfaces and whether the expression of the flagellin and pilin genes, the structural subunits of the flagella and the pili, respectively, is altered after attachment. Shaking *S. solfataricus* P2 cultures were incubated with pieces of mica for two days. Quantitative RT-PCR was performed on cDNA obtained from total mRNAs isolated from planktonic and mica attached cells. Using qPCR we determined that the expression of the flagellin FlaB was 12 fold repressed in attached cells in comparison to planktonic cells whereas the UV induced pilins, UpsA and UpsB, were 5 and 2 fold upregulated, respectively. From the tested 18 genes in the genomic region of SSO3002 - SSO3050 ten genes were not expressed in attached cells whereas eight were clearly induced (Figure 4A and B). Genes strongly induced are predicted to be involved in sugar degradation and metabolism, such as a β-mannosidase (SSO3007), LacS, a β-galactosidase (SSO3019), two carbohydrate transporters (SSO3010/17), a glucose-1 dehydrogenase (SSO3009) and a gluconolactonase (SSO3041). An oxidoreductase (SSO3014) and a dihydrodipicolinate synthase (SSO3035), which is part of the lysine synthesis pathway, were induced as well.

Discussion

In this study we have shown that the hyperthermophilic archaea *S. solfataricus* P2 and PBL2025 are able to attach to a variety of surfaces such as glass, mica, pyrite and carbon-coated gold grids from shaking cultures in a flagella and pili-dependent manner. Cells lacking either the flagella or UV-inducible pili were unable to attach to the tested surfaces. The pili assembled by the *ups* operon so far have only been implicated in cellular aggregation after UV exposure. Our studies demonstrate that these pili are also expressed upon contact with surfaces and that there is an interplay with flagella in surface adhesion. Flagella have also been implicated in mediating surface adhesion and cell-cell contacts in the archaea *P. furiosus* and *M. kandlerii* (Nather et al., 2006, Schopf et al., 2008), but our deletion mutant analysis demonstrates the requirement of these surface structures for attachment from shaking cultures. The qPCR data confirmed that the expression of the UV-induced pilins, UpsA and B, was indeed upregulated in surface attached cells. However, the expression of FlaB was drastically reduced in immobilized cells from which the mRNA for the expression level analysis was isolated after two days incubation.

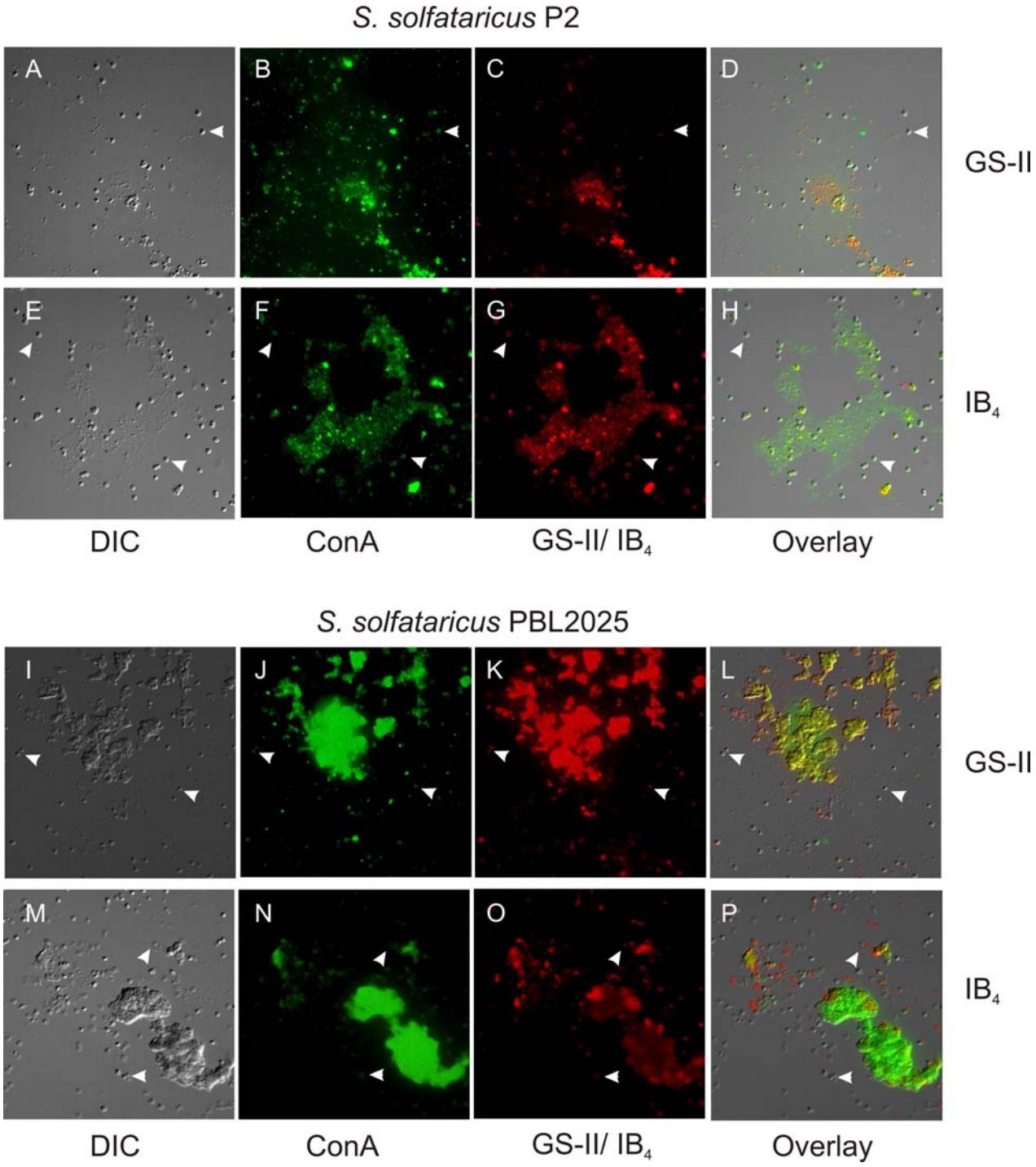

Figure 3. Fluorescent microscopy using fluoresceine coupled ConA (green) and either Alexa coupled GSII or IB4 lectins (both red) on *S. solfataricus* P2 (A-H) and *S. solfataricus* PBL2025 (I-P) attached to glass. A, E,I and M: differential interference contrast; B, F,J, and N: green channel; C, G,K, and O: red channel; D,H,L, and P: overlay of differential interference contrast and fluorescence. White arrowheads indicate the position of cells.

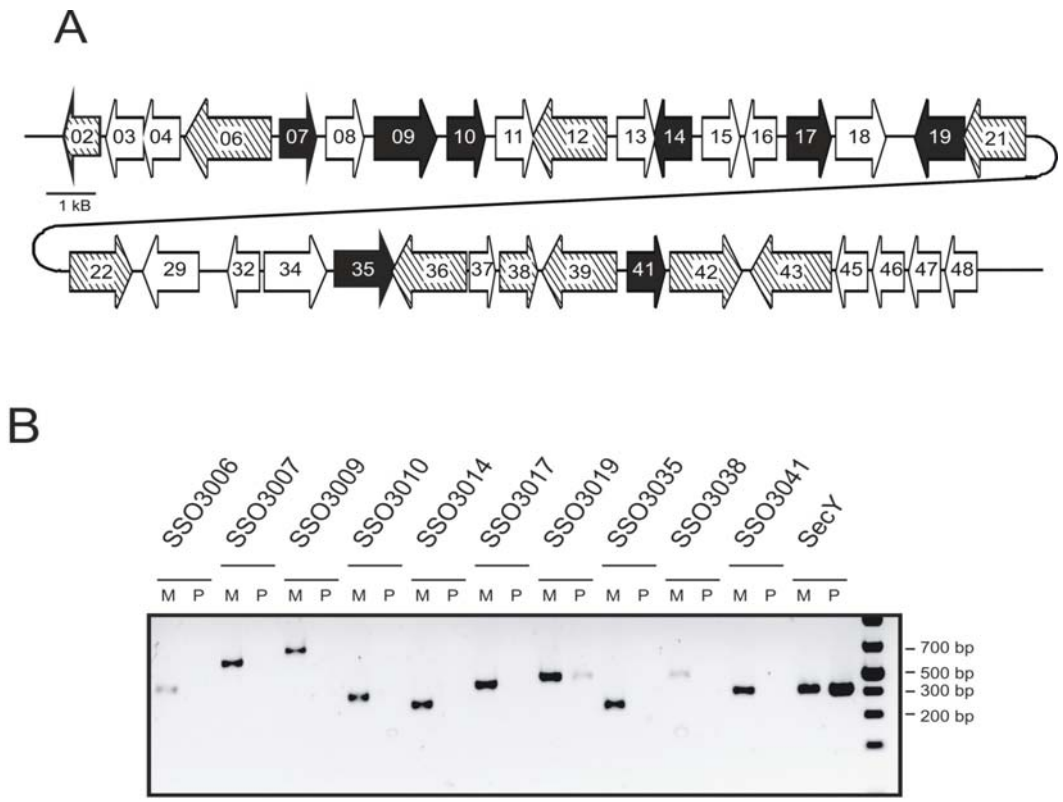

Figure 4. Expression analysis of the genomic region of SSO3002 – SSO3048. A, a schematic view of the genomic region of SSO3002-SSO3048. Genes indicated by hatched arrows were not expressed in attached cells, whereas filled black arrows displayed are induced under sttached conditions. B, agarose gel of RT-PCRs performed on cDNAs from planktonic cells (P) and mica attached cells (M). *secY* was used as a quality control for the isolated RNA and as a housekeeping gene.

Most probably the flagella are necessary for initial attachment and possibly "recognition" of surfaces, but not for persistence once the cells are attached. PBL2025 formed extensive sheets of extracellular material whereas *S. solfataricus* P2 synthesized an extensive network of flagella and pili in order to attach to glass and mica. We utilized fluorescent lectins to study the composition of the EPS formed by these two strains. Glucose, α-D-mannose, α-D-galactose and N-acetyl-D-glucosamine are the minimal component of EPS since a selective reaction was observed with ConA, GS-II and Isolactin IB_4 (Figure 3). This sugar composition matches the sugars found in extracellular glycoproteins of *S. solfataricus* and EPS isolated from shaking *S. solfataricus* MT4 cultures (Elferink et al., 2001b, Nicolaus et al., 2003). We could not observe flagella and Ups pili on mica and glass as clearly as in the transmission electron micrographs from carbon-coated grids. A possible explanation is that both flagella and Ups pili are structural components within the EPS network. A recent study on surface attachment of *E. coli* K12 strain on glass demonstrated that α-D-mannose-rich EPS structures on glass surfaces are essential for the lateral biofilm maturation of the cells (Rodrigues & Elimelech, 2009). The

EPS coat on the hydrophilic glass creates a template for the hydrophobic type 1 fimbriae filaments of *E. coli* and subsequent development of biofilm. In the case of *S. solfataricus*, the EPS is produced in high amount during the attachment of cells on mica and glass, while on carbon-coated grids similar EPS structures were absent. Both glass and mica surfaces are hydrophilic and the carbon films on the EM grids are hydrophobic. One possible explanation is that, *S. solfataricus* EPS creates a template on a hydrophilic surface which is more suitable for other cell surface structures like the S-layer envelope or other glycosylated components of the cell surface during the following development of cells. *S. solfataricus* P2 and PBL2025 differed in the amount and form of the EPS secreted after three days of surface attachment. As PBL2025 lacks a quite large genomic region present in *S. solfataricus* P2 we demonstrated that at least ten of these genes are upregulated upon surface attachment. The majority of these genes are predicted to be involved in sugar degradation and transport. These proteins might be involved in the efficient degradation of the produced EPS or in its modification and modulation, which might explain why with PBL2025 an extensive surface labeling is observed of the EPS. Among the upregulated proteins is LacS, a very well characterized β-galactosidase, and its cognate lactose transporter, which have both been shown to be essential for *S. solfataricus* for growth on lactose (Bartolucci *et al.*, 2003). As we detected glucose and galactosyl residues by lectin staining, lactose might be present as a breakdown product of the EPS. Studies on bacterial EPS in biofilm suggest that glycosylation functions as nutrition storage (Bejarano & Schneider, 2004, Decho & Kawaguchi, 1999, Hassan *et al.*, 2002, Laue et al., 2006, Tsuneda et al., 2003). Therefore, it will be interesting to determine what the purpose is of EPS in archaea and whether it is only composed of sugars or if it contains proteins beside the flagellins and pilins. We have demonstrated that flagella and UV induced pili are essential for initial attachment of *S. solfataricus* and it will be vital to determine which role they play in the development and consolidation of biofilms. Future gene inactivation studies will therefore focus on the role of surface structures, EPS production and degradation in this process.

Table 2. Putative functions of ORFs SSO3002-SSO3048 and induction pattern

ORF number	Putative function	Induced in attached cells
SSO3002	Glycosyltransferase	-
SSO3003	Glucose 1-dehydrogenase	n.d.[1]
SSO3004	3-oxoacyl-(acyl carrier protein) reductase	n.d.
SSO3006	α-mannosidase	-
SSO3007	Endo-β-mannanase	+
SSO3008	Dehydrogenase	n.d.
SSO3009	Carbon monoxide dehydrogenase, large chain	+
SSO3010	Carbohydrate transporter	+
SSO3011	Dehydrogenase	n.d.
SSO3012	ABC-type multidrug transporter	-
SSO3013	Dehydrogenase	n.d.
SSO3014	Oxidoreductase	+
SSO3015	Dehydrogenase	n.d.
SSO3016	Amino hydrolase	n.d.
SSO3017	Carbohydrate transporter	+
SSO3019	β-glycosidase (LacS)	+
SSO3021	Zn-dependent hydrolase	-
SSO3022	α-xylosidase	-
SSO3029	Sugar phosphate isomerase	n.d.
SSO3032	β-xylosidase	n.d.
SSO3034	Hypothetical	n.d.
SSO3035	Dihydrodipicolinate synthase	+
SSO3036	β-glucoronidase	-
SSO3037	Hypothetical	-
SSO3038	Hypothetical	-
SSO3039	Bile acid β-glucosidase	-
SSO3041	Gluconolactonase	+
SSO3042	Glucose dehydronenase	-
SSO3043	ABC transporter, dipeptide binding protein	-
SSO3045	ABC transporter, ATP-binding protein	n.d.
SSO3046	ABC transporter, ATP-binding protein	n.d.
SSO3047	ABC transporter, permease	n.d.
SSO3048	ABC transporter, permease	n.d.

[1] **n.d. not determined**

EXPERIMENTAL PROCEDURES

Strains and growth conditions. *S. solfataricus* P2, *S. solfataricus* PBL2025 (Schelert et al., 2004), ΔflaJ (Szabo et al., 2007a) and ΔupsE (Frols et al., 2007) were grown aerobically at 80°C in the medium described by Brock (Brock et al., 1972), adjusted to pH 3 with sulfuric acid and supplemented with 0.1 % (w/v) of tryptone under moderate agitation. Growth of cells was monitored by measuring the optical density at 600 nm.

Sample preparation for electron microscopy. Samples on 200 mesh carbon-coated gold grids were negatively stained with 2% uranyl acetate and analyzed by transmission electron microscopy on a Philips CM12 (FEI Co., Eindhoven, NL; LaB6 cathode, 120 keV). Samples for scanning electron microscopy were freeze-dried for 2h at -80°C (CFE 50, Cressington Ltd., Watford, UK), rotary shadowed with Platinum/Carbon (1 to 2 nm) and analyzed with a FEI Quanta 400 scanning electron microscope (FEG cathode; 4 to 25 keV).

Fluorescence microscopy. Cells were grown three days in 0.1% tryptone medium in the presence of a glass slide. After cooling down the culture the cells were fixed with 4% formaldehyde for 30 min. The glass slides were washed with Brock medium (pH 5) to remove planktonic cells. Cells on lower side of the glass slides were removed with EtOH. Lectins were applied onto the glass slides, evenly spread with parafilm and incubated for 30 min at room temperature in the dark. Fluorescently labeled lectins used were ConcavalinA (ConA)-fluoresceine conjugate (1 mg/ml), GS-II –Alexa Fluor 594 from Griffonia simplicifolia (1 mg/ml) and GS-IB4-Alexa Fluor 594 from G. simplicifolia (1 mgl/ml). Unbound lectins were removed by washing with Brock medium (pH 5). All lectins were obtained from Molecular Probes. The samples were analyzed by fluorescence microscopy using red filter 750 ms exposure and green filter 250 ms exposure.

Gene expression analysis. *S. solfataricus* P2 cultures were incubated with pieces of mica for two days. Then total RNA was isolated from planktonic cells and cells attached to the mica. Total RNA isolation and cDNA synthesis were performed as described previously (Zolghadr et al., 2007). Gene specific primer sets (table 3) were used to detect the presence of selected genes in the SSO3002-3050 genomic region. PCR products were analyzed on 0.8 % agarose gels. The quantitative PCR analysis was carried out according to the protocol and chemicals provided by Applied Biosystem. For each gene of interest, a duplicate setup of 26 µl PCR mixture was prepared from 13 µl sypro green master mix, 2 µl of 5 µM primer pair stock solution, 2 µl cDNA and 9 µl nucleotide-free water. The negative control assays were done with RNA mixtures that were prepared for cDNA synthesis. Primer efficiencies were calculated from the average slope of the linear regression curves according to the calculation model advised by Applied Biosystem. The fluorescence quantities of the reactions were measured with ABI 7500 instrument (Applied Biosystems, Foster City, CA).

Table 3. Primers used for RT-PCRs and qPCRs

Primer	Sequence (5'-3')
UpsA-rt-forward	**GCTGGGTGGTCTACTTTAT**
UpsA-rt-reverse	**AGTACTGCCCAGCAGTTA**
UpsA-rt-forward	**TCTCACTCATCGTTCCATTA**
UpsA-rt-reverse	**CAGAGTTTCCCTCAATGAAT**
FlaB-rt-forward	**AGACAGCGTCAACAGACTA**
FlaB-rt-reverse	**ACCTGCACTTGTCTGCTGAT**
sso3002-rt-forward	**TGTTGGAGATGGGTGTGATG**
sso3002-rt-reverse	**AGCTGGGTCTGTCGTAATTG**
sso3012-rt-forward	**CCCAACTTCCTCGTTGTTAG**
sso3012-rt-reverse	**TGCCCTCGCAATACTTAACC**
sso3042-rt-forward	**TTTGCGGTACTGATAGGGAG**
sso3042-rt-reverse	**CTGAAGCGCCTGTAGTATCG**
sso3043-rt-forward	**TACTTCACTGACGGCACACC**
sso3043-rt-reverse	**CCGTGGGATTCAAGCAACTG**
SSO3041-rt-forward	**CTGGTCTGCCTGGTTCATAC**
SSO3041-rt-reverse	**CACATCCCTCTGCCTTATTG**
SSO3039-rt-forward	**GAGAAGACTACGCAGTTCCA**
SSO3039-rt-reverse	**GCGTTCCTAGCAACCTCATA**
SSO3036-rt-forward	**CCTATGGGCACCTAAAGGTA**
SSO3036-rt-reverse	**CTGCAACCTCACGTATATCG**
SSO302-rt-forward	**ACTCTAAAGGTCGCTGAGTG**
SSO3021-rt-reverse	**GGAAATTGGCTTGCCTCTTG**
SSO3017-rt-forward	**GGGTGAGTAGGAATAGTAGG**
SSO3017-rt-reverse	**GGAATCAGATAGGGCGTAAG**
SSO3010-rt-forward	**GCGAACTTCGGTTGGTTACT**
SSO3010-rt-reverse	**TACCCACGAGCCTCTGTAAT**
SSO3007-rt-forward	**ATATGATAGGAGCGCGGGAT**
SSO3007-rt-reverse	**CCCTACTTCCTGCTGGATTA**
SSO3014-rt-forward	**CCAGACCCAGATACTCCAAA**
SSO3014-rt-reverse	**CAACATCCTTGAGGCCTAAC**
SSO3038-rt-forward	**TTAGGCGTGTAGGAGGACAA**
SSO3038-rt-reverse	**ACCAGCCATCTATCCCTGAA**
secY-rt-forward	**GGATCGGGAGTTAGTCTGTT**
secY-rt-reverse	**GAAGCTGAGGGTGAGACATA**

Acknowledgements

SVA and BZ were supported by a VIDI grant from the Dutch Science Organization (NWO). SVA was furthermore supported by intramural funds by the Max Planck Society. AK and RR were supported by a grant from the Deutsche Forschungsgemeinschaft.